UNIVERSIDADE ESTADUAL DE CAMPINAS
SISTEMA DE BIBLIOTECAS DA UNICAMP
REPOSITÓRIO DA PRODUÇÃO CIENTIFICA E INTELECTUAL DA UNICAMP

Versão do arquivo anexado / Version of attached file:

Versão do Editor / Published Version

Mais informações no site da editora / Further information on publisher's website:

https://link.springer.com/article/10.1007/s13538-020-00842-y

DOI: 10.1007/s13538-020-00842-y

Direitos autorais / Publisher's copyright statement:

©2021 by Springer. All rights reserved.

DIRETORIA DE TRATAMENTO DA INFORMAÇÃO

Cidade Universitária Zeferino Vaz Barão Geraldo
CEP 13083-970 – Campinas SP
Fone: (19) 3521-6493
http://www.repositorio.unicamp.br

Brazilian Journal of Physics
https://doi.org/10.1007/s13538-020-00842-y

A Tutorial Review on Time-Frequency Analysis of Non-Stationary Vibration Signals with Nonlinear Dynamics Applications

Marcus Varanis[1] · **Anderson L. Silva**[2] · **José M. Balthazar**[3] · **Robson Pederiva**[4]

Received: 4 September 2020 / Accepted: 2 December 2020
© Sociedade Brasileira de Física 2021

Abstract

Time-frequency analysis (TFA) for mechanical vibrations in non-stationary operations is the main subject of this article, concisely written to be an introducing tutorial comparing different time-frequency techniques for non-stationary signals. The theory was carefully exposed and complemented with sample applications on mechanical vibrations and nonlinear dynamics. A particular phenomenon that is also observed in non-stationary systems is the Sommerfeld effect, which occurs due to the interaction between a non-ideal energy source and a mechanical system. An application through TFA for the characterization of the Sommerfeld effect is presented. The techniques presented in this article are applied in synthetic and experimental signals of mechanical systems, but the techniques presented can also be used in the most diverse applications and also in the numerical solution of differential equations.

Keywords Time-frequency analysis · Non-stationary signals · Sommerfeld effect · Nonlinear jump · Nonlinear dynamics

CWT	Continuous wavelet transform
DOF	Degree of freedom
Dmeyer	Discrete wavelet Meyer Filter
EMD	Empirical mode decompostion
FFT	Fast Fourier transform
Fs	Sampling frequency
FT	Fourier transfomr
FSST	Short-time Fourier transform-based synchrosqueezing transform
HT	Hilbert transform
HHT	Hilbert-Huang transform
HSA	Hilbert spectral analysis
MEMS	Micro-electro-mechanical systems
SE	Spectral entropy
SK	Spectral kurtosis
SST	Synchrosqueezed transform
STFT	Short-time Fourier transform
TFA	Time-frequency analysis
TRF	Time-frequency representation
WSST	Wavelet-based synchrosqueezing transform
WVD	Wigner–Ville distribution

1 Introduction

With the spread of microcomputer-based and, more recently, open platform-based data acquisition systems [27, 46, 70, 83, 109–111], beyond the use of MEMS sensors to measure mechanical measurements [24, 45, 108], these works generally use the Arduino microcontroller and Raspberry Pi single-board computers with sensors such as accelerometer, gyroscope, ultrasound, and infrared, to instrument vibrations in mechanical systems. These tools are available to a wide range of students, professionals, and young researchers in various areas of knowledge. On the other hand, while in dedicated systems all the signal processing was done by proprietary software or hardware, without major user intervention and/or knowledge, in generic or open platform-based data acquisition systems

---

✉ Marcus Varanis
marcusvaranis@ufgd.edu.br

[1] Faculty of Engineering, Federal University of Grande Dourados, Rodovia Dourados-Itahum, Km 12, S/N, Dourados, MS, Brazil

[2] Mechanical Engineering Department, Federal University of Paraná, Av. Cel. Francisco H. dos Santos, 230, Jardim das Américas, Curitiba, PR, Brazil

[3] Federal University of Technology - Paraná, R. Doutor Washington Subtil Chueire, S/N, Jardim Carvalho, Ponta Grossa, PR, Brazil

[4] School of Mechanical Engineering, University of Campinas, Rua Mendeleyev, 200, Cidade Universitária “Zeferino Vaz” Barão Geraldo, Campinas, SP, Brazil

Published online: 03 January 2021

it is the user who implement the computational routines that calculate the spectra and other parameters of the acquired signals. One of the objectives of this tutorial is to present time-frequency analysis techniques for the processing of digitized signals in a microcomputer with special attention to the application in linear and nonlinear mechanical systems, particularly to mechanical vibration signals.

Spectral analysis techniques based on Fourier transform through FFT are efficient for analysis of signals with stationary characteristics; however, many random processes are non-stationary, causing frequencies to change over time. Thus, the signal misses the periodic characteristic, one of the basic assumption for the use of the Fourier transform [2, 21, 71].

Furthermore, systems excited by non-ideal power sources, such as numerous motors, may exhibit some nonlinear phenomena in their response, such as the Sommerfeld effect and the jump phenomenon. These phenomena occur due to nonlinear interactions between energy sources and elastic systems. In the occurrence of these phenomena, frequency jumps occur in the system response and the increase and/or decrease of the vibration amplitude. Processing signals of this nature need more specific techniques, as there are large concentrations of energy in the time-frequency domain that eventually hide frequencies with less energy.

According to Addison [2], various signals from machines and mechanical components have non-stationary characteristics, such as stopping and starting signals from electric motors. Stop and start signals are particularly interesting because they capture the richer frequency spectrum and effectively store all the spectral information of the signal [107, 121]. In these cases, the Fourier transform becomes inadequate for the frequency domain signal representation. In stationary signal analysis, the concept of amplitude and frequency spectrum is generally intuitive [90]; for non-stationary operation, it is more difficult to determine the amplitude or frequency of the signal, since these quantities may vary over time, so it is helpful to introduce the concept of instantaneous amplitude and frequency. These concepts are widely used through the Hilbert transform [30, 90]. To deal with these issues, time and frequency domain representation methods are often combined into a single representation, which presents how the spectral content of a signal evolves over time and is a more appropriate tool for non-stationary signal analysis [28, 30, 86]. It is emphasized, for example, that the characterization of failures in a mechanical system is made by observing changes in the signal frequency spectrum [107]. Also, the feature extraction of images and neurophysiological and speech signals can be realized through the characterization of the signal energy, in a simple and precise way [33]. The time-frequency decomposition [2] maps a 1-D signal to a 2-D time and frequency image and provides information about local frequency variations. The literature presents a large number of methods for this purpose, categorized mainly as linear or quadratic methods [28, 36, 114]. The linear methods include notably STFT and CWT, while the quadratic methods, such as spectrogram, scalogram, and WVD, that treat the signal-associated power spectral density [18]. A detailed and rigorous study on the subject can be found at [11, 28].

One of the techniques used in non-stationary signal analysis is the short-time Fourier transform (STFT). In this case, the signal is placed in two dimensions, time and frequency. It is known that in the analysis made from STFT there is a compromise between time and frequency. Signal analysis gives information on when and which frequencies vary. However, this information is limited to the size of the window, which once set will be the same for all frequencies [28]. In [73], the basic concept of STFT is used but the size of the window is fixed in the frequency domain instead of the time domain. This approach is simpler than similar existing methods, such as adaptive STFT and multi-resolution STFT; it emphasizes that the method proposed by the authors requires neither a band-pass filter banks nor the evaluation of local signal characteristics of adaptive techniques.

Another widely used technique for signal analysis in non-stationary and transient operations is the Wigner-Ville distribution (WVD), which is part of a group of integral transforms called bilinear. This technique was the first attempt to perform a joint time and frequency analysis [72]. The bilinear Wigner-Ville distribution achieves better time-frequency domain joint resolution compared to any linear transform; however, it suffers from a cross-term interference problem, which does not represent any signal information, i.e., the WVD of two signals is not the sum of their individual WVDs [72].

In this context of time-frequency analysis is proposed the wavelet transform in order to overcome the window limitation of the STFT formulation, and overcome the interference problems of the Wigner-Ville distribution and deficiencies of other methods based on integral transforms [21, 107, 127]. An important feature of the Wavelet transform is that the frequency resolution varies in proportion to the center frequency variation. For the past two decades, the Wavelet transform has been successfully used in the most diverse areas of scientific knowledge and especially in mechanical system applications, as well as many other fields of engineering, with proven success in non-stationary signal analysis. The Wavelet transform is applied in several studies with relative success. This can be seen in the work of Yan and Gao [127], where they demonstrate various techniques based on the wavelet transform for fault diagnosis in rotating machines. Several other works use techniques based on Wavelet transform for fault detection in mechanical systems [16, 34, 90, 105, 107, 127, 130], in structural dynamics and structural health [4, 19, 38, 44, 49, 68, 92], and in nonlinear dynamics applications [50, 85, 102–104, 112, 124, 125]. In [85] was studied the nonlinear dynamics of a shape memory oscillator subjected to ideal and non-ideal excitations. The numerical results show that the CWT scale index can successfully detect the system behavior when the signal presents chaotic behavior.

Another emergent technique for time-frequency analysis with wide application in mechanical systems is the Hilbert-Huang transform (HHT), this technique is a way of decompose a signal into so-called intrinsic mode functions together with a trend and obtaining data from instantaneous frequency. The method is designed to work well with non-stationary and nonlinear data [39–41]. In contrast to other common transforms, such as the Fourier transform, HHT is a similar algorithm and has an empirical approach that can be applied to a dataset rather than a theoretical tool. The HHT is based on the empirical mode decomposition (EMD) and Hilbert transform (HT); thus, it is an empirical analysis method and its expansion base is adaptive, so that it can produce physically significant results in the analysis of nonlinear and non-stationary signals. The advantage of being an adaptive method comes at a price: the difficulty of a theoretical foundation [41]. HHT has wide application in mechanical systems analysis such as failure analysis in rotating systems [15, 47, 56, 116, 128], parameter identification [3, 51, 61, 77, 88], and nonlinear dynamics [13, 14, 17, 32, 42, 63, 80].

Another technique widely used in TFA is spectral kurtosis (SK), which has been introduced as a statistical tool that can indicate not only non-Gaussian components in a signal but also their frequency domain locations. It was initially used as a complement to the power spectral density and demonstrated its efficiency in problems related to the transient detection in noisy signals. The literature presents successful applications in vibration-based condition monitoring with the use of SK [5, 118]. Several application examples of the use of SK can be seen in [35, 57, 64, 66, 89, 113]. A rigorous study can be found at [93].

New time-frequency analysis techniques have been proposed in recent years. An emerging technique is the synchrosqueezed transform. Known limitations, such as tradeoffs between time and frequency resolution, can be overcome by alternative techniques that extract instantaneous modal components, as presented in the synchrosqueezed transforms. The EMD of a signal into components that are well separated in the time-frequency domain allows the reconstruction of these components [6, 79, 123]. In particular, the work presented in [6] provides an overview of time-frequency reassignment and synchronization techniques used in multicomponent signals, covering theoretical history and applications, and attempts to explain how synchrosqueezing can be viewed as a special case of rebuilding the reassignment enable mode. Synchrosqueezing transform-based methods are actually an extension of the CWT that incorporates empirical mode decomposition elements and frequency reassignment techniques. This new tool produces a better defined time-frequency representation, allowing instantaneous frequency identification to highlight individual components.

Wavelet-based synchrosqueezing transform (WSST) is a time-frequency analysis method proposed by Daubechies and Maes in 1996 [22]. In 2011, Daubechies et al. [23] propose a combination method through wavelet analysis and EMD relocation method. By introducing a precise mathematical definition for a class of functions that can be seen as an overlay of a fairly small number of roughly harmonic components and proving that our method actually succeeds in decomposing arbitrary functions in this class. The anti-noise capability and time-frequency resolution of the WSST are enhanced based on the wavelet transform (WT). WSST maintains the advantages of EMD and CWT. WSST is adaptive like EMD and does not depend on the mother wavelet. The problem of mixing modes is significantly improved. Nowadays, WSST has been deeply applied to mechanical systems with applications as parameter estimation [53, 71, 74, 75, 84, 119, 120, 129], Rotor Rub-Impact Fault Diagnosis [65, 101, 117], structural dynamics [62, 71, 84], and characterization of chaotic behavior in several nonlinear systems [69, 96, 104, 117, 126]. In [37], a new stochastic chaotic secure communication scheme based on the WSST algorithm is proposed.

About other recent works on SST , we can mention the demodulation transform-based SST method (also called instantaneous frequency-embedded-SST) was introduced in [48, 58, 115] to change the instantaneous frequency (IF) of signal so that more accurate IF estimation and component recovery (mode retrieval) can be achieved. Adaptive FSST and adaptive WSST were proposed and analyzed in [60, 67, 94] and [9, 12, 59] respectively. In these papers, the window width of the continuous wavelet for WSST and the window function for FSST are time-varying. The results presented in the literature demonstrate these methods outperform the conventional WSST and FSST.

In addition, for the improvement of current machines, nonlinear investigation of their dynamics is necessary and this point is especially important when it comes to rotating machines. It is observed that when it is considered that a nonlinear motor exciting a structure has limited power and its rotation depends on the response of the structure to which it is coupled, the resultant electromechanical system presents a much richer dynamic than the linear case, being possible to identify the most diverse nonlinear effects [7, 8, 20, 76].

A very notable phenomenon is the Sommerfeld effect, which occurs in systems that are at some point excited at their resonant frequencies by a non-ideal power source. In this phenomenon, the power source cannot transform all incoming energy into useful work and transforms a fraction of this energy into mechanical vibration [20, 31]. Thus, the Sommerfeld effect causes large vibration amplitudes to the system, which can damage the structure due to the high stresses generated.

However, it is known that algorithms based on the Fourier transform are not indicated for nonlinear signal analysis, so for nonlinear phenomenon identification in mechanical systems it is necessary to use signal processing techniques applicable to nonlinear signals with good time and frequency domain resolution.

In particular, this tutorial consists of presenting applications of time-frequency analysis in synthetic and experimental signals of mechanical systems, but the techniques presented can also be used in the most diverse applications and also in the numerical solution of differential equations. The independent variable is generally assumed to be the time, but nothing prevents to be a spatial variable or any other quantity.

This paper is divided into some sections for better organization of the topics. Section 2 presents the methodologies used for the time-frequency representations realized in this paper. Section 2.1 presents the short-time Fourier transform, Section 2.2 introduces the wavelet transform, Section 2.3 discusses the Hibert-Huang transform, and Section 2.4 discusses the syncrosqueezed transforms. Section 3 presents the case studies covered by this paper, being divided into synthetic test signals, Section 3.1, and experimental test signals, Section 3.2; altogether, four case studies were performed in this paper. Section 4 presents the results obtained and Section 5 presents the conclusions and final remarks.

2 Time-Frequency Representation Methodology

2.1 Short-Time Fourier Transform

STFT is the most commonly used method for studying non-stationary and transient signals due to its simplicity and computational power. The basic idea of the method is to divide the signal into several short time blocks that are separated or overlapped and then perform the FT on each block. This is done by multiplying the signal analyzed by a family of models obtained through time translation and frequency modulation of a window function [90]. In (1), we present the expression of STFT where the signal $x(t)$ is previously "windowed" by a $g(t)$ function, around a τ time.

$$STFT(\tau, f) = \int_{-\infty}^{\infty} x(t)g(t-\tau)e^{-i2\pi ft}dt \tag{1}$$

The magnitude spectrum, spectrogram, can be obtained by:

$$S(\tau, f) = \left|\int_{-\infty}^{\infty} x(t)g(t-\tau)e^{-i2\pi ft}dt\right|^2 \tag{2}$$

There is a trade-off between time and frequency in the STFT. In [1], a study is carried out comparing the efficiency of the STFT in separating the components of a signal for different window lengths. The signal analysis gives information on when and which frequencies vary. However, this information is limited to the window length, which once set will be the same for all frequencies. A more generic formulation can be found in [86] and a more detailed and mathematically rigorous formulation in [6, 28].

2.2 Continuous Wavelet Transform

The CWT was proposed in order to overcome the limitation of the window length in STFT. The wavelet transform uses a variable window, where the resolutions vary along the time-frequency plane, so as to obtain all the information contained in the signal [2]. Equation (3) presents the wavelet transform in the continuous form (CWT).

$$W(a, b) = \int_{-\infty}^{\infty} x(t)\bar{\psi}_{a,b}(t)dt \tag{3}$$

where,

$$\bar{\psi}_{a,b}(t) = \frac{1}{\sqrt{(a)}}\bar{\psi}\left(\frac{t-b}{a}\right) \tag{4}$$

In (4), the term $\bar{\psi}(t)$ is the prototype of windows, known in wavelet theory as the mother wavelet. The factor$\frac{1}{\sqrt{a}}$ ensures the normalization of energy to any scale. This analysis determines the correlation of the $x(t)$ signal through translations τ and changes of scales, for a given wavelet mother. Criteria for choosing the mother wavelet are found in [107]. In mechanical vibration analysis, Daubechies and Meyer discrete wavelets are successfully used [105–107]

2.3 Hilbert-Huang Transform

According to Huang [39], Hilbert-Huang transform (HHT) is a TFA method that can be divided into two steps: In the first, there is the EMD process, which allows an adaptive set of base functions to be obtained, and the second, through the HSA, allows obtaining a time-frequency domain representation by calculating the Hilbert transform of each of the functions obtained by EMD analysis.

The two main steps of HHT are [81]:

1. Apply EMD to decompose a time domain signal into n intrinsic mode functions c_i corresponding to different intrinsic time scales as follows:

$$u(t) = \sum_{i=1}^{n} c_i(t) + r_n \tag{5}$$

   the term r_n in (5) denotes the residue.
2. Apply the Hilbert transform and calculate the time-dependent frequency and amplitude A_i of each term c_i.

   The intrinsic mode function is a function that satisfies two conditions:

   - The number of extremes and the number of zero crossings must be the same or different from one in all data.
   - The envelope defined by the local minimum and maximum must be symmetrical, and therefore the average value of the maximum envelope and the minimum envelope is 0 at any given point. Once the extremes are identified, all local maxima are interpolated by a cubic spline as the upper envelope. The procedure for the local minimums to produce the lower envelope is then repeated. The average of the upper and lower envelopes is designated as m_{11}, and the first intrinsic function c_{11} is given by:

$$c_{11} = u(t) - m_{11} \tag{6}$$

The sifting process has to be repeated more times. In the kth sifting process, c_{1k-1} is treated as the data, then [81].

$$c_{1k} = c_{1k-1} - m_{1k} \tag{7}$$

were $k = 2, ..., K$. The process is repeated until all local maxima are positive, all local minima are negative, and the waves are almost symmetrical, so c_{1k} is accepted as c_1. One systematic method for ending the iteration is to limit the D_v deviation calculated from the two consecutive sifting results as follows:

$$D_v = \sqrt{\frac{\sum_{i=1} N(c_{1k}(t_i) - c_{1k}(ti))^2}{\sum_{i=1}^{N} c_{1k-1}^2(t_i)}} \tag{8}$$

In (8), $t_i = i\delta t$ and $N\delta t = T$ denote the sampled period. Once you get c_1, then set the residue r_1, treat r_1 as the new data, and repeat the steps in (6) and (7) as follows:

$$\begin{aligned} c_{21} &= r_1 - m_{21}, \quad r_1 \equiv u(t) - c_1 \\ c_{2k} &= c_{2k-1} - m_{2k} \end{aligned} \tag{9}$$

$k = 2, \ldots, K$. After obtaining the term c_2, the residue r_2 is defined and the steps are repeated as in (10).

$$\begin{aligned} c_{31} &= r_2 - m_{31}, \quad r_2 \equiv u(t) - c_1 - c_2 \\ c_{3k} &= c_{3k-1} - m_{3k}, \quad k = 2, \ldots, K \end{aligned} \tag{10}$$

After determining all the terms $c_i(t)$, the Hilbert transform can be applied to get $d_i(t)$ from each term c_i. Thus, it is defined:

$$\begin{aligned} z_i(t) &= c_i(t) + jd_i(t) = A_i e^{j\theta_i} \\ A_i &= \sqrt{c_i^2 + d_i^2}, \quad \theta_i(t) = \frac{\tan^{-1} d_i}{c_i}, \quad \omega_i = \frac{d\theta_i}{dt} \end{aligned} \tag{11}$$

Replacing $c_i(t)$ in (5) with $z_i(t)$ in (11) and neglecting r_n yield:

$$u(t) = Real\left(\sum_{i=1}^{n} A_i(t) e^{j\theta(t)_i}\right) \tag{12}$$

Where

$$\theta(t)_i = \int_0^t \omega_i(t)dt = arctan\left(\frac{d_i}{c_i}\right) \tag{13}$$

HHT is an adaptive method and intrinsic mode functions are generally physical because the characteristic scales are physical. Since distorted harmonics with time-dependent frequencies and amplitudes are allowed in data decomposition, spurious harmonics are not required to represent non-stationary and nonlinear signals [40, 81]. In addition, EMD essentially acts as an adaptive filter bank. A more detailed and mathematically rigorous formulation can be found in [40, 43].

2.4 Synchrosqueezed Transform

STFT and CWT are the main approaches for simultaneously decomposing a signal into time and frequency components. Known limitations, such as trade-offs between time and frequency resolution, can be overcome by alternative techniques that extract instantaneous modal components. EMD aims to break down a signal into components that are well separated in the time-frequency plane, allowing the reconstruction of these components [6]. On the other hand, a recently proposed method called synchrosqueezing transform (SST) is an extension of the wavelet transform that incorporates empirical mode decomposition elements and frequency reassignment techniques. This new tool produces a well-defined time-frequency representation, allowing the identification of instantaneous frequencies in non-stationary signals to highlight individual components [6, 123].

The SST was initially proposed for the Wavelet transform [23] and then later extended to the STFT [6]. In fact, it corresponds to a nonlinear operator that emphasizes the time-frequency representation of a signal by combining the location and dispersion properties of the reassignment methods with the invertibility property of the linear time-frequency representations [23].

2.4.1 Wavelet-Based Synchrosqueezing Transform

Wavelet-based synchrosqueezing transform, proposed by Daubechies et al. [23], is basically composed of three steps. The first step is to calculate CWT according to Eq. (3). In the second step, a preliminary $\omega_s(a,b)$ frequency is obtained from the oscillatory behavior of $W_s(a,b)$ in a, such that:

$$\omega_s(a,b) = -i\,(W_s(a,b))^{-1}\,\frac{\partial}{\partial b}W_s(a,b) \tag{14}$$

In the third step, the time scale plane is transformed to the time-frequency plane. Each value of $W_s(a,b)$ is reassigned to (a,ω_l), where ω_l denotes the frequency that is closest to the preliminary frequency of the original (discrete) point $\omega_s(a,b)$. This operation is presented in Eq. (13) [74]:

$$T_s(\omega_l,b) = (\Delta\omega)^{-1} \sum_{a_k:|\omega(a_k,b)-\omega_l|\le\Delta\omega/2} W_s(a_k,b)a_k^{-3/2}\,(\Delta a)_k \tag{15}$$

In Eq. (14), $\Delta\omega$ is the width of each frequency bin $\Delta\omega = \omega_l - \omega_{l-1}$ and equivalently for Δb.

SWT can obtain a high-resolution time-frequency spectrum by compressing (reassigning) the CWT result. However, when the amplitude of the high-frequency components of a signal is low, it is difficult to identify the components in the CWT spectrum or the SST spectrum that is based on the CWT result. In contrast to CWT, the SWT transform is able to more efficiently display the high-frequency and low-amplitude components of a signal and perform a lossless reverse transformation, but the ST resolution is not yet satisfactory [23, 84].

Originally proposed in the case of wavelet, the SST was extended similarly to the STFT context, known as STFT-based SST. This method was first proposed and studied in [100, 122]. A mathematically more rigorous formulation can be found in [6, 79, 123].

3 Case Studies

3.1 Synthetic Test Signals

3.1.1 Case 1: Multicomponent Signal Analysis

In this first application was studied multicomponent signals, that is, wave modulation overlays that appear in many physical systems, especially in mechanical systems. To facilitate replicability and comparison with other methods, a set of two synthetic multicomponent signals is initially considered, with 100, 001 samples, sampling frequency (Fs) equal to 1000 Hz, and duration of 10 s. The signals with the addition of +30 dB of additive white Gaussian noise.

The first signal consists of two linear chirps to show the linear rate of change of frequency as a function of time. The first chirp has $f_0 = 50$ Hz, $f_1 = 400$ Hz. Since the second chirp has $f_0 = 400$ Hz, $f_1 = 50$ Hz, this model is also known as cross chirp signal (Fig. 1a) [11, 97].

The second signal consists of the sum of three linear chirps, a model known as divergent chirp signal (Fig. 1b) [91], each showing the linear rate of change of frequency as a function of time. The first component has $f_0 = 0$ Hz, $f_1 = 400$ Hz. The second component has $f_0 = 0$ Hz, $f_1 = 200$ Hz, while the third component has $f_0 = 0$ Hz and $f_1 = 100$ Hz.

3.1.2 Case 2: 1DOF Syntentic Mechanical System

The resonance phenomenon is commonly found in nature. In electrical and mechanical systems, it occurs when two different energy storage devices have equal (but opposite signals) impedances. During resonance, energy is passed back and forth between the two energy storage devices. The signal shown in Fig. 5a is from a 1DOF mechanical system with resonant frequency $wn = 39,789$ Hz, being excited by variable sinusoidal $(0 - 160$ Hz) for 5 s. The signal has $F_s = 1000$ Hz.

3.2 Experimental Test Signals

The measured signals obtained by the most diverse sensors during dynamic events generally contain nonlinear, non-stationary, and noisy properties. In this work was utilized experimentally obtained acceleration signals from two mechanical systems with 1 and 3 DOF, which have their experimental and data acquisition procedure carefully described in [102, 111].

3.2.1 Case 3: Experimental 1DOF System

The system under study with 1DOF [102] consists of a portico with 400 mm width and 300 mm height. Its sides are made of ASTM A-36 steel and the lower and upper floors are made of polypropylene (Nitapro®). The steel plates that make up the sides have dimensions of 76.2 × 300 mm and 1.75 mm thickness, while the polypropylene plates have dimensions 76.2 × 400 mm and 15 mm thickness. The lower floor is considered rigid and fixed to the ground. At the top of the portico, there is an unbalanced DC motor with a mass of 6.59 g and a radius of 15 mm. The Sommerfeld effect occurs due to a nonlinear interaction between the motor speed and the dynamic response of the portico. In this system, the Sommerfeld effect occurs at its second natural frequency, 45 Hz. A detailed description of the experimental apparatus can be found at [102].

Signals are obtained through an accelerometer attached to the side of the portico at its upper end. A Type 4508 Brüel & Kjær accelerometer was used, which can work in a temperature range of −54 to 121 °C and is capable of measuring frequencies from 0.3 to 8 kHz. Utilized were a Brüel & Kjær signal conditioner and the National Instruments USB-6251 signal acquisition system [102]. The signals were acquired with a sampling frequency of 1000 Hz and 32,768 points, totaling an acquisition time of 32,768 s. These signals are transient signals of the motor starting with a small permanent at the end, where the motor speed is varied from 0 to 20 Hz where there is no Sommerfeld effect (Fig. 7a), and 0 to 65 Hz where the Sommerfeld effect is present (Fig. 7b).

3.2.2 Case 4: Experimental 3DOF System

The system under study [102, 111] consists of a three degree of freedom (3 DOF) shearbuilding structure, which has a width of 400 mm and a height of 900 mm. Its sides are made of ASTM A-36 steel and the floors are made of polypropylene (Nitapro®). The steel plates that compose the sides have dimensions of 76.2 × 300 mm and 1.75 mm of thickness, while the polypropylene plates have dimensions 76.2 × 400 mm, 15 mm of thickness, and are equally spaced 300 mm apart. The lower floor is considered rigid and fixed to the ground. At the top of the shearbuilding, there is an unbalanced DC motor with a mass of 6.59 g and a radius of 15 mm. The Sommerfeld effect occurs due to a nonlinear interaction between engine speed and shearbuilding dynamic response. In this system, the Sommerfeld effect occurs at 45 Hz [102].

Signals are obtained through an accelerometer attached to the side of the portico at its upper end. A Type 4508 Brüel & Kjær accelerometer was used, which can work in a temperature range of −54 to 121 °C and is capable of measuring frequencies from 0.3 to 8 kHz. Utilized were a Brüel & Kjær signal conditioner and the National Instruments USB-6251 signal acquisition system [102]. The signals were acquired with a sampling frequency of 1000 Hz and 32,768 points, totaling an acquisition time of 32,768 s. These signals are transient signals of the motor starting with a small permanent at the end, where the motor speed is varied from 0 to 20 Hz where there is no Sommerfeld effect (Fig. 11a), and 0 to 65 Hz where the Sommerfeld effect is present (Fig. 11b).

4 Results

In this section are presented the results of the case studies presented in Section 3, presenting the temporal signals, obtained either numerically or experimentally, and their respective time-frequency representations, which are described in Section 2.

4.1 Synthetic Test Signals

4.1.1 Case 1: Multicomponent Signal Analysis

Figure 1 presents the analysis of the chirps described in Section 3 (Fig. 1a and b) using STFT using a 256-sample Hann window (Fig. 1c and d) and through CWT using Bump wavelet (Fig. 1e and f). The representation through STFT was adequate for the analysis of both chirps, and their spectral contents are well represented as shown in Fig. 1c and d.

Both analyses, STFT and CWT, have good time-frequency domain representation and correctly show the linear rate of change in frequency of the two chirps as a function of time. Note in the STFT analysis that Gaussian noise is also well represented in the analysis of both chirps. The codes for STFT Matlab® implementations can be found at [10, 11, 28], in Python [26, 52, 54].

Figure 2a and b show the analysis realized by means of the CWT using the Meyer wavelet, while Fig. 2c and d show the analysis realized with the WPT using the DMeyer filter. In this CWT analysis, using the Meyer wavelet, we can observe the good representation of the spectral content and less energy dispersion in the time-frequency representation.

In the WPT analysis was utilized the DMeyer filter and the decomposition was done until the 8th level. This level already guarantees an adequate resolution in the time-frequency representation in this specific case. The DMeyer filter is known to be especially efficient for chirping and transient analysis [107], as observed in the results obtained (Fig. 2c and d). CWT and WPT Matlab® implementation codes can be found at [10, 87, 90, 95, 98]. Python can be found in [29, 54, 55, 78, 82].

Figure 3 presents the analyses made through HHT, using cubic spline interpolation [40]. The use of HHT allows high resolution in the time and frequency domain, as shown in Fig. 3a and b, but the HHT method is very sensitive to noise. For HHT implementation in Python, the PYHHT library can be used [25].

Figure 4 shows the analysis made through FSST (Fig. 4a and b), and analysis through WSST (Fig. 4c and d). It is apparent in both synchrosqueezed transform-

Fig. 1 Time-Frequency Analysis by means of the STFT and CWT: **a** Cross Chirp signal, **b** Divergent Chirp signal, **c** STFT of cross chirp **d** STFT of divergent chirp **e** CWT of cross chirp signal and **f** CWT of divergente chirp signal

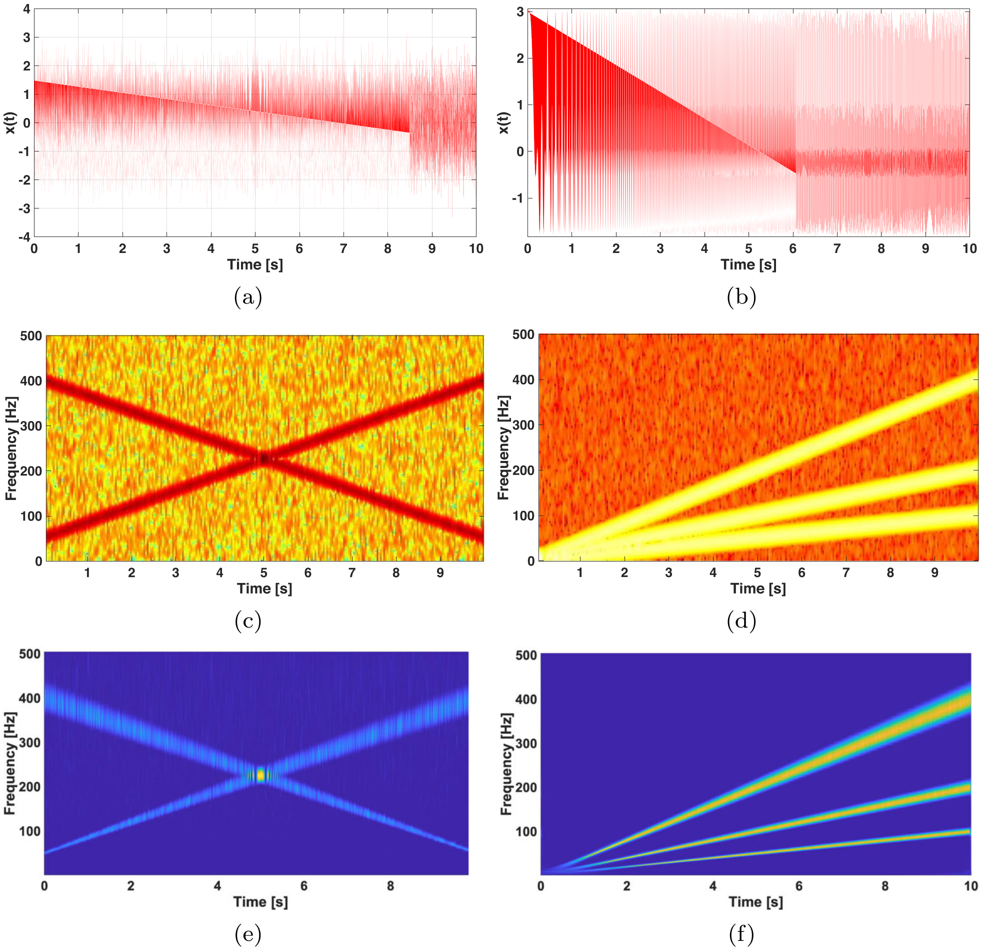

(a) (b) (c) (d) (e) (f)

Fig. 2 Time-frequency analysis using CWT and WPT: **a** CWT of cross chirp signal, **b** CWT of divergent chirp signal, **c** WPT of cross chirp, and **d** WPT of divergent chirp

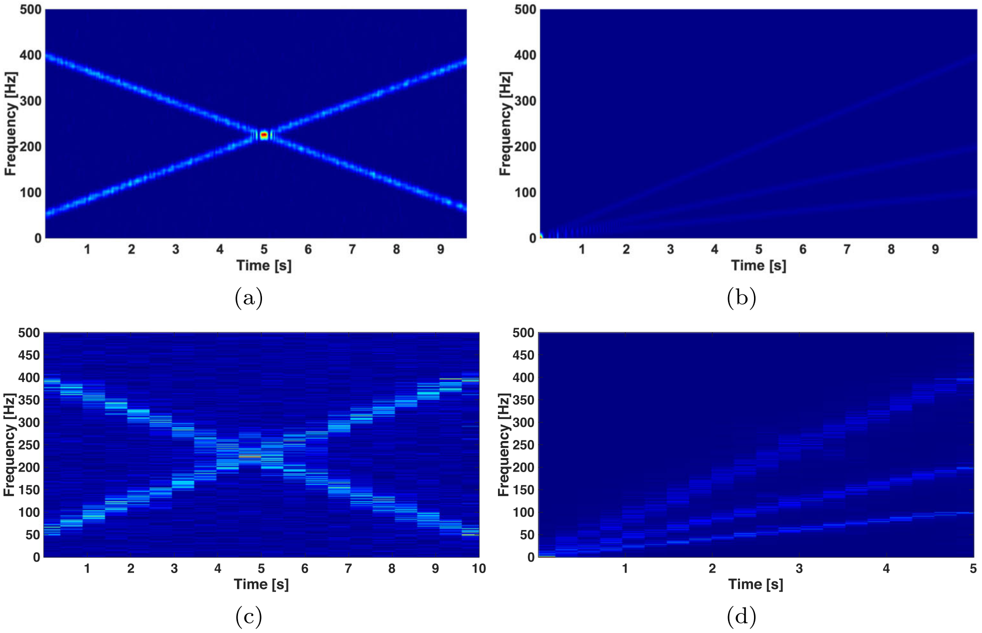

(a) (b) (c) (d)

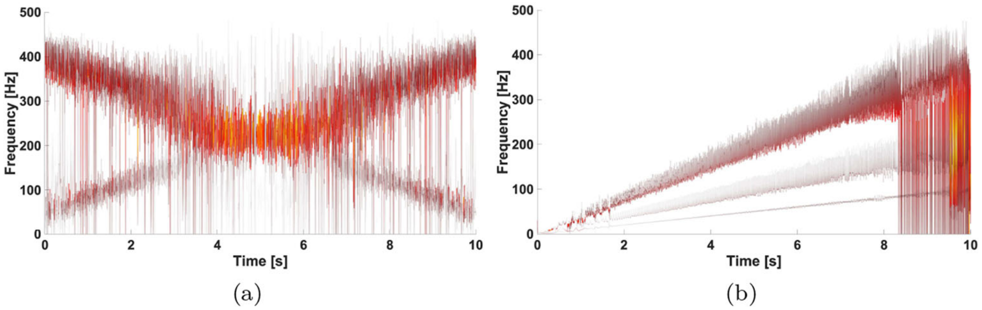

(a)

(b)

Fig. 3 Time-frequency analysis by means of the HHT: **a** HHT of the cross chirp signal, **b** HHT of the divergent chirp signal

based analyses that the energy dispersion in the time-frequency plane is much smaller than in the other cases, demonstrating excellent resolution in the time-frequency domain. Matlab® implementations can be found at [99].

4.2 Case 2: 1DOF syntentic Mechanical System

Figure 5 presents the analysis of the 1 DOF mechanical system described in Section 3. The analysis performed through STFT is presented in Fig. 5b and c using CWT with the bump wavelet. In Fig. 5d, the result obtained through the Meyer wavelet is presented. In STFT analysis, a Hann window with 256 sample length was used. In all cases the resonant frequency, $f_n = 39,789$ Hz, is well characterized; however, the CWT analyses present the energy more concentrated in the system resonant frequency on the time-frequency domain, which makes the characterization most effective.

Figure 6 presents the analysis of the 1DOF mechanical system through the application of WPT, HHT, FSST and WSST. In WPT analysis, Fig. 6a, it is possible to characterize the resonant frequency of the system, and even with a significant energy dispersion in the time-frequency domain due to the excitation signal, its characterization is still quite proper. The HHT analysis clearly characterizes the resonant frequency. Figure 6c and d are performed the analysis via FSST and WSST. Again it is possible to observe in both analyzes using the synchrosqueezed transform techniques that the energy dispersion in the time-frequency plane is much smaller than in the other cases, with excellent resolution in the time and frequency domain. The use of the WSST method proved to be much more appropriate.

4.3 Experimental Test Signals

4.3.1 Case 3: 1DOF Experimental Mechanical System

In this section, the experimental signals presented in Fig. 7 come from a portal frame mechanical system, which has a degree of freedom, briefly described in Section 3 and detailed in [102]. The objective of this analysis is to characterize the resonance phenomenon and the Sommerfeld effect in the time and frequency domains.

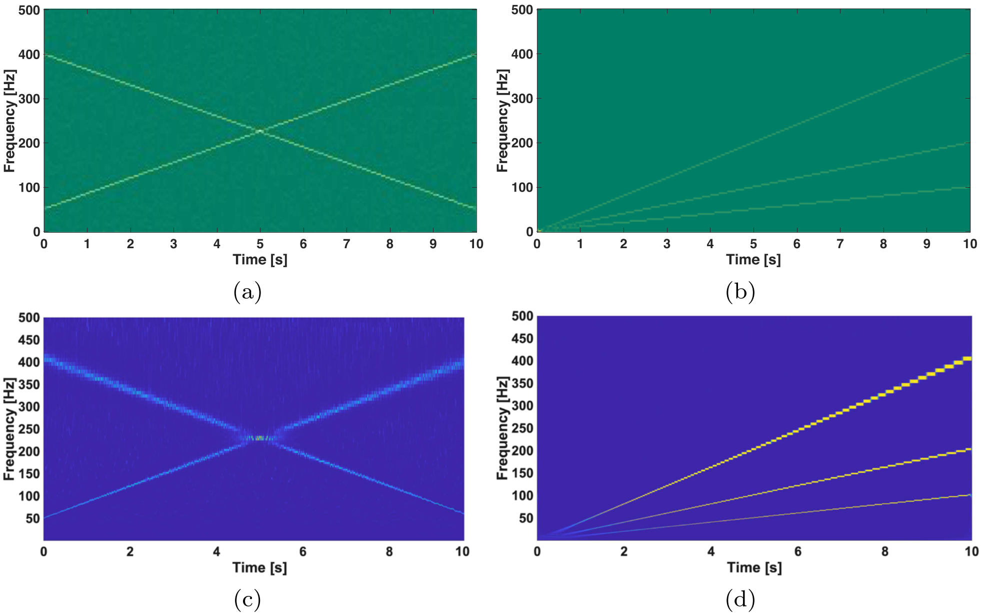

(a)

(b)

(c)

(d)

Fig. 4 Time-frequency analysis using FSST and SWT: **a** FSST of cross chirp signal, **b** FSST of divergent chirp signal, **c** WSST of cross chirp, and **d** WSST of divergent chirp

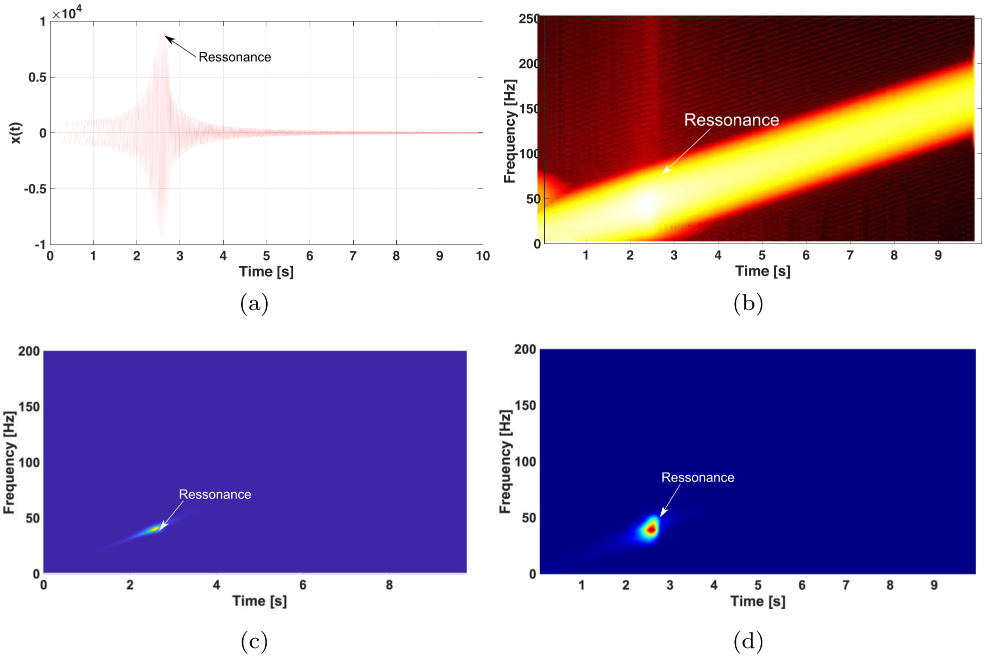

Fig. 5 Time-frequency analysis using STFT and CWT: **a** 1DOF syntentic mechanical system signal, **b** STFT 1DOF syntentic mechanical system, **c** CWT using bump wavelet 1DOF syntentic mechanical system, **d** CWT using Meyer wavelet 1DOF syntentic mechanical

Figure 7 also presents the system time-frequency analyses by applying STFT (Fig. 7c and d).

Figure 7c shows the presence of several harmonics in the signal, but the most energetic presence related to the motor acceleration signal is highlighted, in addition to the presence of the system resonant frequency, in a point where there is the highest concentration of energy. Already in Fig. 7d it is possible to observe that besides the presence of the harmonics and the first natural frequency of the system, there is also a greater concentration and dispersion of energy in the time-frequency plane, coming from Sommerfeld effect and jump phenomena. Despite the dispersion of energy in the time-frequency spectrum in both analyses performed with the STFT, it is noted the very energetic presence of the first natural frequency. In Fig. 7c at about 9 s, there is a large energy concentration near the frequency

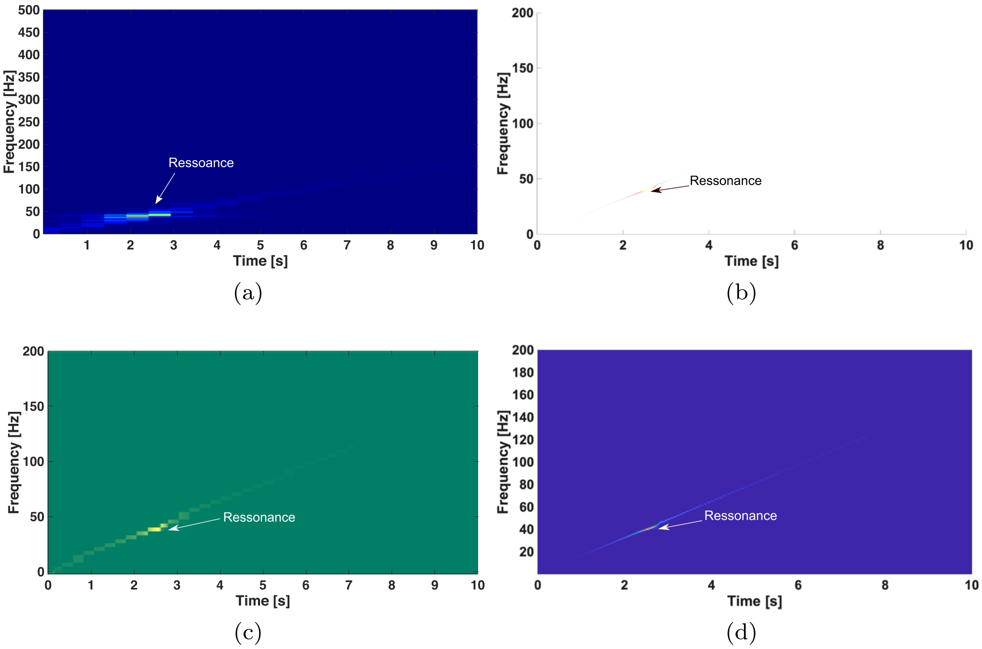

Fig. 6 Time-frequency analysis 1DOF syntentic mechanical system using WPT, HHT, FSST, and WSST: **a** WPT using Dmeyer filter 1DOF syntentic mechanical system signal, **b** HHT 1DOF syntentic mechanical system, **c** FSST 1DOF syntentic mechanical system, and **d** WSST using Meyer wavelet 1DOF syntentic mechanical

Fig. 7 Time-frequency analysis using STFT: **a** 1DOF experimental mechanical system signal without Sommerfeld effect, **b** 1DOF experimental mechanical system signal with Sommerfeld effect, **c** STFT 1DOF experimental mechanical system signal without Sommerfeld effect, **d** STFT 1DOF experimental mechanical system signal with Sommerfeld effect

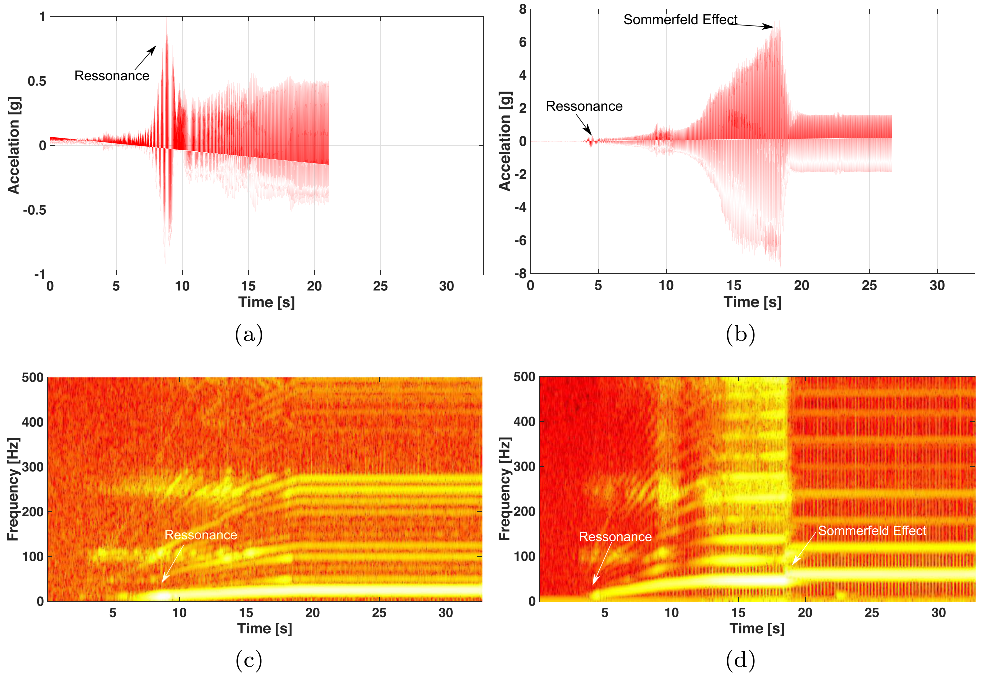

of 11 Hz and in Fig. 7c there is a concentration of energy at the same frequency, now at 4 s, in addition to a high-energy concentration at a frequency of 45 Hz between 15 and 19 s due to the resonance capture phenomenon and energy dispersion before the frequency jumps to 60 Hz at 19 s due to the jump phenomena.

The analysis presented in Fig. 8a and b deals with the application of CWT using the Morlet wavelet to signals. Additionally, it is also analyzed through the use of WPT using Dmey filter in Fig. 8a and b. In the CWT analysis in Fig. 8a, the resonant frequency is clearly identified as in the STFT analysis at 9 s with a value of approximately 11 Hz as well as the entire operating regime of the motor. In Fig. 8b, there is no spectrum dispersion as shown in [102], but the characteristic jump phenomenon of the Sommerfeld Effect is clearly observed, with energy concentration at 45 Hz between 14 and 19 s with a jump to the frequency of 60 Hz at 19 s. Already the analysis

Fig. 8 Time-frequency analysis using CWT and WPT: **a** CWT 1DOF experimental mechanical system signal without Sommerfeld effect, **b** CWT 1DOF experimental mechanical system signal without Sommerfeld effect, **c** WPT 1DOF experimental mechanical system signal without Sommerfeld effect, **d** WPT 1DOF experimental mechanical system signal with Sommerfeld effect

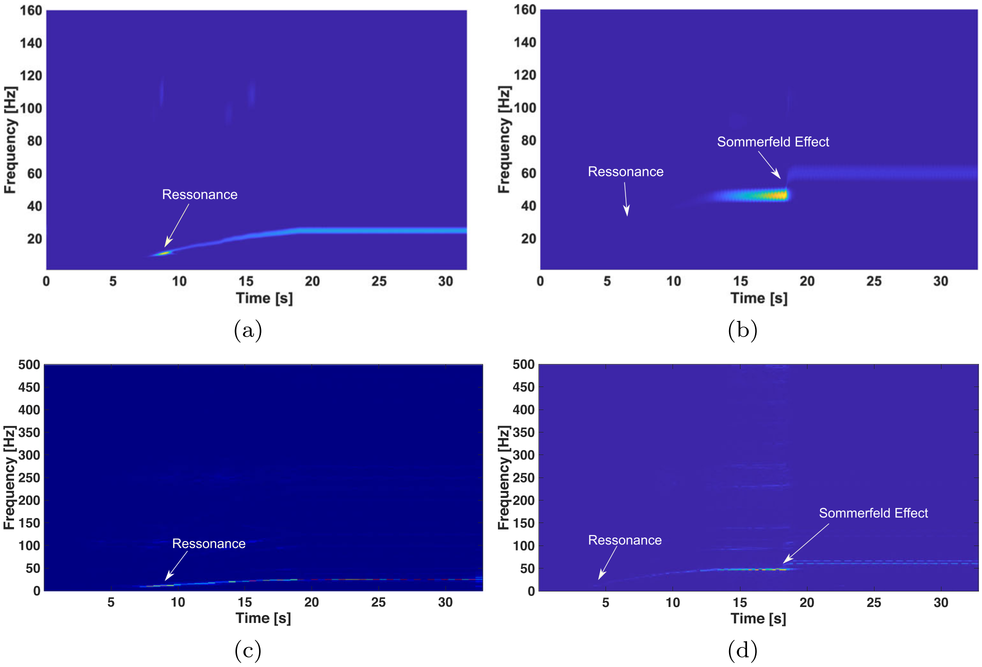

made through WPT shows in Fig. 8c the presence of harmonic frequencies in the signal, but the frequencies related to the resonant frequency of the system and the operating regime of the motor are clearly more energetic. It is also noted that the packet related to the first natural frequency is more energetic than the others. Figure 8d shows that the first natural frequency of the system does not have relevant energy in the analysis, while a dispersion of energy over the time-frequency plane is highlighted, with significant concentration of energy in the packet related to the frequency of 45 Hz, which characterizes the Sommerfeld effect and the jump phenomena.

Figure 9 presents time-frequency analyses using HHT; the results can be viewed in Fig. 9a and b. High resolution in the frequency domain is observed. The resonance phenomenon is well characterized in Fig. 9a at 9 s, as well as the Sommerfeld effect in Fig. 9b at 19 s of analysis.

Finally, Fig. 10 presents the analysis based on the synchrosqueezed transform methods, using FSST and WSST. The results of the 1 DOF Experimental mechanical system analysis without sommerfeld effect signal are presented in Fig. 10a and c. The results of the analysis of the system with Sommerfeld effect are presented in Fig. 10b and d. In both cases, the resonance phenomenon and the Sommerfeld effect are well characterized with good energy concentration in the time-frequency distribution, most notably the presence of the 11 Hz frequency in the analysis without the Sommerfeld effect while the jump phenomenon is well characterized in both methods. Both techniques are quite suitable for the proposed problem type, highlighting that the analysis performed by WSST presents higher energy concentration, which allows a better identification of the frequencies present in the signal.

4.4 Case 4: 3DOF Experimental Mechanical System Signal

In this section, the experimental signals shown in Fig. 11a and b are derived from a shearbuilding mechanical system with a 3-DOF, previously described in Section 3 and detailed in [102, 111].

Figure 11c and d present the system time-frequency analysis through the application of STFT. Figure 11c shows a large presence of noise in the analysis, but even so the system signal has a reasonable representation; it is possible to identify the moment of occurrence of the resonance of the third mode of vibration of the system, at 10 s with the value of 20 Hz, which is the most energetic mode of the system. However, due to the large energy dispersion in the time-frequency plane, it is not possible to identify the other resonant frequencies of the system. Figure 11d presents the analysis of the signal with the Sommerfeld effect. Again, the noise representation is clear, as is the system's response to engine operation. The third resonant frequency of the system stands out, at approximately 6 s with a value of 20 Hz, but the first two are not distinguished. In addition, the Sommerfeld effect is clearly noted due to the energy concentration between 15 and 20 s at the frequency of 45 Hz and the dispersion of power and the sudden increase in the frequency of the signal to 60 Hz at 20 s.

Figure 12 presents the results based on the wavelet transform by applying CWT to the system (Fig. 12a and b), and WPT (Fig. 12c and d). In the case without the Sommerfeld effect, the signal energy is concentrated in the third natural frequency of the system, 20 Hz at 15 s, due to its greater amplitude. In the case of the presence of the Sommerfeld effect, the signal energy is divided with the frequency in which the resonance capture phenomenon occurs, 45 Hz between 15 and 20 s, so both frequencies are highlighted in the analysis. WPT analysis using the DMeyer filter shows a lower concentration of energy in the frequencies mentioned above, distributing the energy throughout the signal, enabling to identify not only the third resonant frequency and the Sommerfeld effect, but also all the variation of the signal frequency over time.

Figure 13 presents the time-frequency analysis of the time series of the 3DOF experimental mechanical system through the use of HHT; the results can be viewed in Fig. 13a and b. In the case analysis without the Sommerfeld effect, the system's third resonant frequency, 20 Hz at 10 s, and the operating range of the motor are characterized. In the case with the Sommerfeld effect, we can also observe

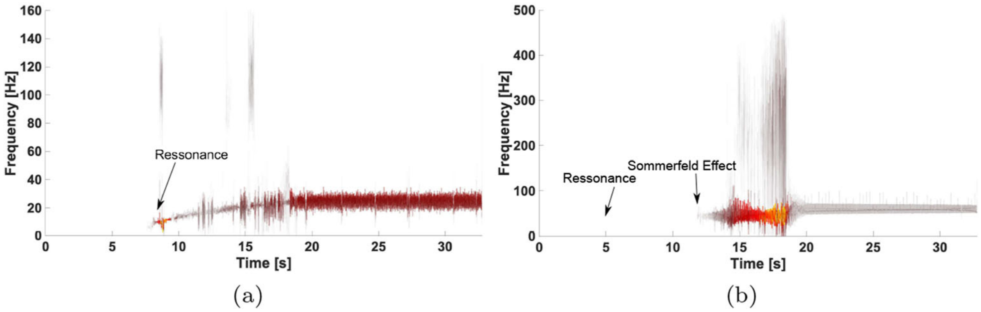

(a) (b)

Fig. 9 Time-frequency analysis via HHT: **a** HHT 1DOF experimental mechanical system signal without Sommerfeld effect, **b** HHT 1DOF experimental mechanical system signal with Sommerfeld effect

Fig. 10 Time-frequency analysis using synchrosqueezed transform: **a** FSST 1DOF experimental mechanical system signal without Sommerfeld effect, **b** FSST 1DOF experimental mechanical system signal without Sommerfeld effect, and **c** WSST 1DOF Experimental mechanical system signal without Sommerfeld effect and **d** WSST 1DOF experimental mechanical system signal with Sommerfeld effect

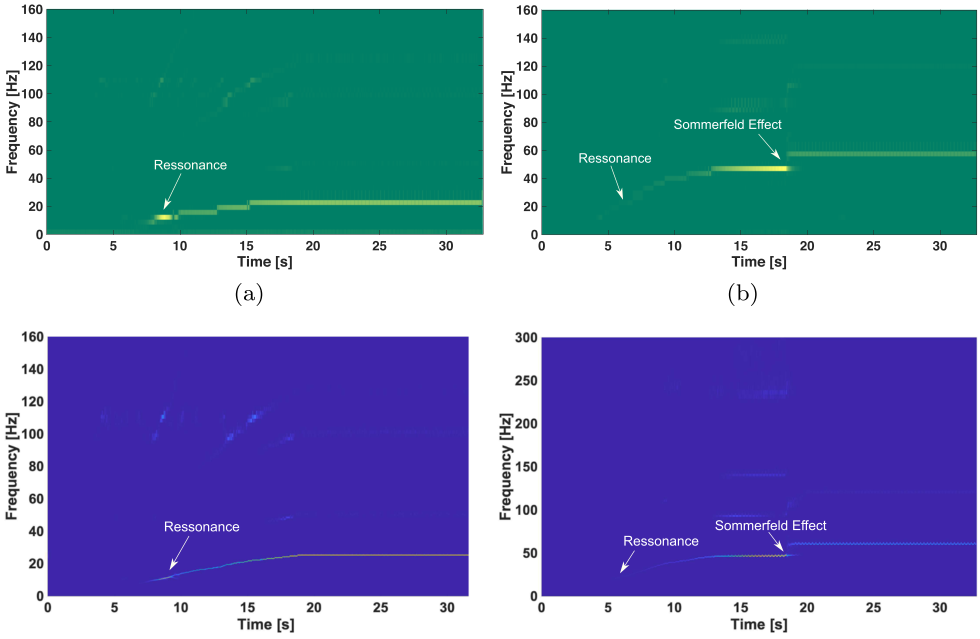

(a) (b)

(c) (d)

the third resonant frequency of the system, 20 Hz at 6 s, and all the phenomena related to the Sommerfeld effect, which occur at a frequency of 45 Hz at 20 s.

Figure 14 presents the analysis based on the synchrosqueezed transform methods through the use of FSST and WSST. The results of the 3DOF experimental mechanical system analysis without Sommerfeld effect signal are presented in Fig. 14a and b. The results of the analysis of the system with Sommerfeld effect are presented in Fig. 14c and d. Again, there is less energy dispersion by the time-frequency plane, and it is possible to identify the second and third resonant frequencies of the system in the case without the Sommerfeld effect, respectively 13 Hz at 10 s and 20 HZ at 15 s, occurring subtly in the analysis with FSST and more clearly in the case of WSST. Even in the case that the Sommerfeld effect is present, it is possible to identify the

Fig. 11 Time-frequency analysis using STFT: **a** 3DOF experimental mechanical signal system without Sommerfeld effect, **b** 3DOF experimental mechanical signal system with Sommerfeld effect, **c** STFT 3DOF experimental mechanical signal system without Sommerfeld effect, and **d** STFT 3DOF Experimental mechanical system signal with Sommerfeld effect

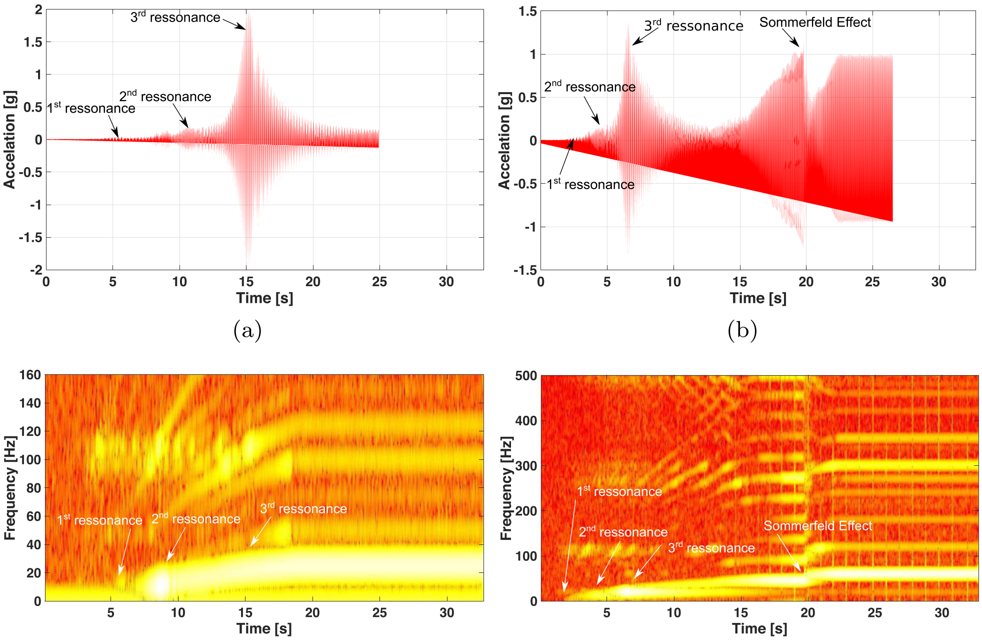

(a) (b)

(c) (d)

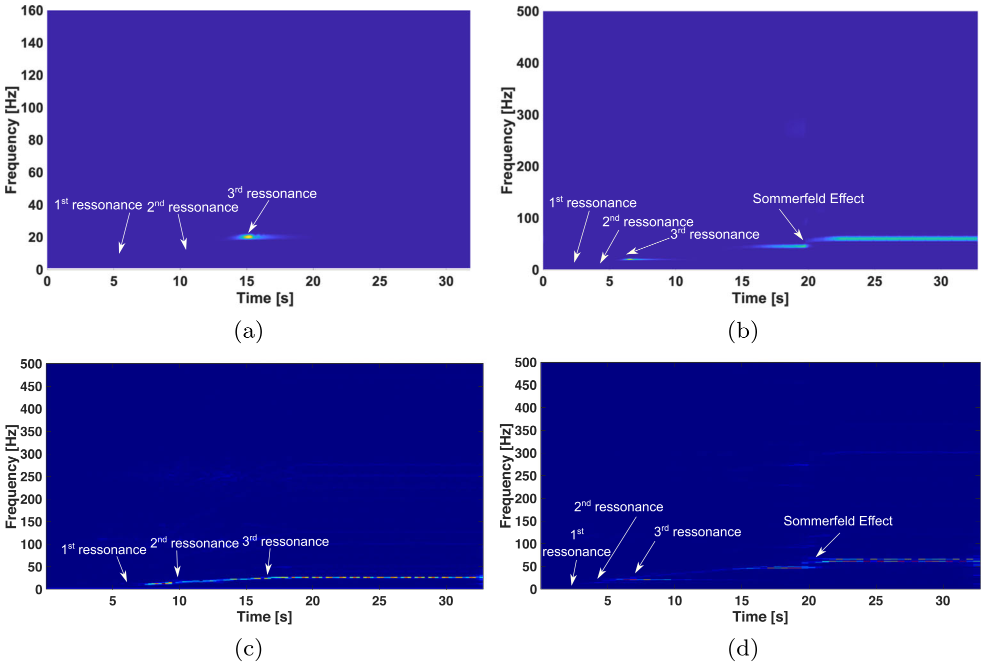

(a) (b) (c) (d)

Fig. 12 Time-frequency analysis using CWT and WPT: **a** CWT 3DOF experimental mechanical system signal without Sommerfeld effect, **b** CWT 3DOF experimental mechanical system signal with Sommerfeld effect, **c** WPT 3DOF experimental mechanical system signal without Sommerfeld effect, and **d** WPT 3DOF experimental mechanical system signal with Sommerfeld effect

second and third resonant frequencies of the system, respectively, 13 Hz at 4 s and 20 Hz at 6 s, and the effects due to the nonlinearities of the system, which occur between 16 and 20 s at the frequency of 45 Hz and 60 Hz, which demonstrates the low-energy dispersion capacity of the SST, which allows the representation of less energetic frequencies with excellent resolution.

5 Conclusions

In this paper was investigated several current techniques for non-stationary signal processing, particularly in the study of mechanical vibrations, evaluating their efficiency in separating frequency components, such as in the evaluation of case studies involving chirps, and in identifying frequencies with different energy levels. The STFT is applicable to the studied signals, but presents results with low resolution in the time-frequency plane and it has large energy dispersion, which makes it difficult to identify lower energy frequencies. It may also have resolution issues because of the fixed size of the window.

Wavelet transform-based techniques, CWT and WPT, present good resolution in the time-frequency plane, but CWT still obfuscates other components when there are high-energy concentrations at some signal frequency. WPT, with the use of Dmey filter and decomposition to the 8th level, presented better results in these cases, being possible to distinguish several signal components. Applications of wavelet transform-based techniques to non-stationary

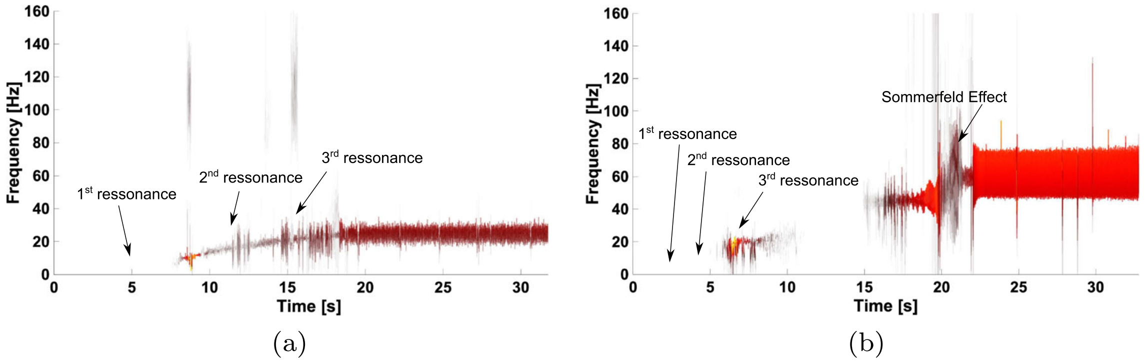

(a) (b)

Fig. 13 Time-frequency analysis via HHT: **a** 3DOF HHT experimental mechanical system signal without Sommerfeld effect, **b** 3DOF HHT experimental mechanical system signal with Sommerfeld effect

Fig. 14 Time-Frequency Analysis Using synchrosqueezed transform: **a** FSST 3DOF Experimental mechanical system signal without Sommerfeld effect, **b** FSST 3DOF Experimental mechanical system signal with Sommerfeld effect, **c** WSST 3DOF Experimental mechanical system signal without Sommerfeld effect and **d** WSST 3DOF Experimental mechanical system signal with Sommerfeld effect

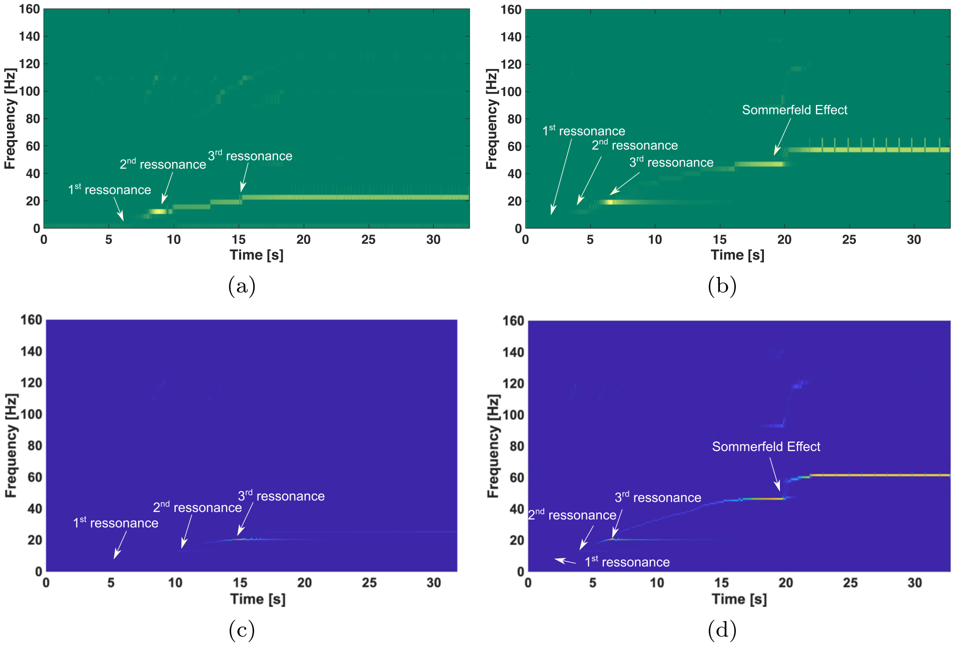

(a) (b) (c) (d)

signals have demonstrated the ability of this technique to monitor signal frequency variations and to detect short-term transients with excellent time-frequency localization, far exceeding the limitations presented by the techniques based on the Fourier transform.

The application of HHT to the studied signals was also satisfactory, but in the steady state of the motor in the experimental results its resolution was not so great, being not possible to have a value for the signal frequency in this period. In this application, the method was very sensitive to noise.

Finally, the results obtained through the SSTs were excellent, presenting an optimal time-frequency resolution and minimum energy dispersion. Although both SST techniques have shown good results, it is observed that those obtained through WSST have better resolution than FSST, being possible to identify the signal frequency at any time. Thus, the results show that SSTs present better results in the proposed application, with special emphasis on WSST, which presents better resolution in the time-frequency domain.

The results showed the benefits through this approach for structural dynamics analysis and non-stationary operation problems, where the use of time-frequency analysis techniques was quite adequate and easy to apply. The results presented in this paper indicate the great potential of these tools for the characterization of nonlinearities in mechanical systems, especially the use of WPT and WSST.

References

1. Limitations of the fourier transform: Need for a data driven approach. https://pyhht.readthedocs.io/en/latest/tutorials/limitations_fourier.html. Accessed: 2019-12-20
2. P.S. Addison, *The illustrated wavelet transform handbook: introductory theory and applications in science, engineering, medicine and finance* (CRC press, Boca Raton, 2017)
3. J.P. Amezquita-Sanchez, H.S. Park, H. Adeli, A novel methodology for modal parameters identification of large smart structures using music, empirical wavelet transform, and hilbert transform. Eng. Struct. **147**, 148–159 (2017)
4. J. Andre, A. Kiremidjian, Y. Liao, C. Georgakis, R. Rajagopal, Structural health monitoring approach for detecting ice accretion on bridge cable using the haar wavelet transform. in *Sensors and Smart Structures Technologies for Civil, Mechanical, and Aerospace Systems 2016, vol. 9803, p. 98030F. International Society for Optics and Photonics*, (2016)
5. J. Antoni, The spectral kurtosis: a useful tool for characterising non-stationary signals. Mech. Syst. Signal Process. **20**(2), 282–307 (2006)
6. F. Auger, P. Flandrin, Y.T. Lin, S. McLaughlin, S. Meignen, T. Oberlin, H.T. Wu, Time-frequency reassignment and synchrosqueezing: An overview. IEEE Signal Process. Mag. **30**(6), 32–41 (2013)
7. J.M. Balthazar, J.L.P. Felix, R.M.F. Brasil, Short comments on self-synchronization of two non-ideal sources supported by a flexible portal frame structure. Modal Anal. **10**(12), 1739–1748 (2004)
8. J.M. Balthazar, D.T. Mook, H.I. Weber, R.M. Brasil, A. Fenili, D. Belato, J. Felix, An overview on non-ideal vibrations. Meccanica **38**(6), 613–621 (2003)
9. A. Berrian, N. Saito, Adaptive synchrosqueezing based on a quilted short-time fourier transform. in *Wavelets and Sparsity*

XVII. International Society for Optics and Photonics, Vol. 10394, (2017), p. 1039420
10. K. Blinowska, J. Zygierewicz, *Practical biomedical signal analysis using MATLAB* (CRC Press, Boca Raton, 2011)
11. B. Boashash, *Time-frequency signal analysis and processing: a comprehensive reference* (Academic Press, Cambridge, 2015)
12. H. Cai, Q. Jiang, L. Li, B.W. Suter, Analysis of adaptive short-time fourier transform-based synchrosqueezing transform. arXiv:1812.11033 (2018)
13. M. Candon, R. Carrese, H. Ogawa, P. Marzocca, C. Mouser, O. Levinski, Characterization of a 3dof aeroelastic system with freeplay and aerodynamic nonlinearities–part ii: Hilbert–huang transform. Mech. Syst. Signal Process. **114**, 628–643 (2019)
14. E.S. Carbajo, R.S. Carbajo, C. Mc Goldrick, B. Basu, Asdah: An automated structural change detection algorithm based on the hilbert–huang transform. Mech. Syst. Signal Process. **47**(1-2), 78–93 (2014)
15. N.H. Chandra, A. Sekhar, Fault detection in rotor bearing systems using time frequency techniques. Mech. Syst. Signal Process. **72**, 105–133 (2016)
16. J. Chen, Z. Li, J. Pan, G. Chen, Y. Zi, J. Yuan, B. Chen, Z. He, Wavelet transform based on inner product in fault diagnosis of rotating machinery: A review. Mech. Syst. Signal Process. **70**, 1–35 (2016)
17. G.J. Clarke, S.S. Shen, Hilbert–huang transform approach to lorenz signal separation. Adv. Adapt. Data Anal. **7**(01n02), 1550004 (2015)
18. L. Cohen, Vol. 778, *Time-frequency analysis* (Prentice Hall, Upper Saddle River, 1995)
19. L. Comerford, H. Jensen, F. Mayorga, M. Beer, I. Kougioumtzoglou, Compressive sensing with an adaptive wavelet basis for structural system response and reliability analysis under missing data. Comput. Struct. **182**, 26–40 (2017)
20. L. Cveticanin, M. Zukovic, J.M. Balthazar, *Dynamics of mechanical systems with non-ideal excitation* (Springer, Berlin, 2018)
21. I. Daubechies, Vol. 61, *Ten lectures on wavelets* (SIAM, Philadelphia, 1992)
22. I. Daubechies, A nonlinear squeezing of the continuous wavelet transform based on auditory nerve models. Wavelets Med. Biol., 527–546 (1996)
23. I. Daubechies, J. Lu, H.T. Wu, Synchrosqueezed wavelet transforms: An empirical mode decomposition-like tool. Appl. Comput. Harmon. Anal. **30**(2), 243–261 (2011)
24. G. D'Emilia, D. Di Gasbarro, A. Gaspari, E. Natale, Identification of calibration and operating limits of a low-cost embedded system with mems accelerometer. in *Journal of Physics: Conference Series*, Vol. 882 (IOP Publishing, 2017), p. 012006
25. J. Deshpande, pyhht documentation (2018)
26. A.B. Downey, *Think DSP: digital signal processing in Python.* (O'Reilly Media Inc., Sebastopol, 2016)
27. T.T. Duc, T. Le Anh, H.V. Dinh, Estimating modal parameters of structures using arduino platform. in *International Conference on Advances in Computational Mechanics* (Springer, 2017), pp. 1095–1104
28. P. Flandrin, *Explorations in time-frequency analysis* (Cambridge University Press, Cambridge, 2018)
29. G. Lee, R. Gommers, F. Wasilewski, K. Wohlfahrt, A. O'Leary, H. Nahrstaedt, Contributors, PyWavelets - Wavelet Transforms in Python. https://github.com/PyWavelets/pywt [Online; accessed 2018-12-20] (2006)
30. J.M. Giron-Sierra, *Digital signal processing with matlab examples, volume 1: signals and data, filtering, non-stationary signals, modulation* (Springer, Berlin, 2016)
31. P. Gonċalves, M. Silveira, B.P. Junior, J. Balthazar, The dynamic behavior of a cantilever beam coupled to a non-ideal unbalanced motor through numerical and experimental analysis. J. Sound Vib. **333**(20), 5115–5129 (2014)
32. A. González, H. Aied, Characterization of non-linear bearings using the hilbert–huang transform. Adv. Mech. Eng. **7**(4), 1687814015582120 (2015)
33. R.C. Guido, A tutorial on signal energy and its applications. Neurocomputing **179**, 264–282 (2016). https://doi.org/10.1016/j.neucom.2015.12.012. http://www.sciencedirect.com/science/article/pii/S0925231215019281
34. W. Guo, L. Huang, C. Chen, H. Zou, Z. Liu, Elimination of end effects in local mean decomposition using spectral coherence and applications for rotating machinery. Digit. Signal Process. **55**, 52–63 (2016)
35. D. He, X. Wang, S. Li, J. Lin, M. Zhao, Identification of multiple faults in rotating machinery based on minimum entropy deconvolution combined with spectral kurtosis. Mech. Syst. Signal Process. **81**, 235–249 (2016)
36. F. Hlawatsch, F. Auger, *Time-frequency analysis* (Wiley Online Library, New York, 2008)
37. J. Hu, L. Chai, D. Xiong, W. Wang, A novel method of realizing stochastic chaotic secure communication by synchrosqueezed wavelet transform. Digit. Signal Process. **82**, 194–202 (2018)
38. C. Huang, C. Liu, W. Su, Application of cauchy wavelet transformation to identify time-variant modal parameters of structures. Mech. Syst. Signal Process. **80**, 302–323 (2016)
39. N.E. Huang, Vol. 16, *Hilbert-Huang transform and its applications* (World Scientific, Singapore, 2014)
40. N.E. Huang, Introduction to the hilbert–huang transform and its related mathematical problems. in *Hilbert–Huang transform and its applications*, (World Scientific, 2014), pp. 1–26
41. N.E. Huang, N.O. Attoh-Okine, *The Hilbert-Huang transform in engineering* (CRC Press, Boca Raton, 2005)
42. N.E. Huang, K. Hu, A.C. Yang, H.C. Chang, D. Jia, W.K. Liang, J.R. Yeh, C.L. Kao, C.H. Juan, C.K. Peng, et al., On holo-hilbert spectral analysis: a full informational spectral representation for nonlinear and non-stationary data. Philos. Trans. A Math. Phys. Eng. Sci. **374**(2065), 20150206 (2016)
43. N.E. Huang, Z. Shen, S.R. Long, M.C. Wu, H.H. Shih, Q. Zheng, N.C. Yen, C.C. Tung, H.H. Liu, The empirical mode decomposition and the hilbert spectrum for nonlinear and non-stationary time series analysis. in *Proceedings of the Royal Society of London A: mathematical, physical and engineering sciences*, Vol. 454 (The Royal Society, 1998), pp. 903–995
44. F. Huda, I. Kajiwara, N. Hosoya, Damage detection in membrane structures using non-contact laser excitation and wavelet transformation. J. Sound Vib. **333**(16), 3609–3624 (2014)
45. M. Iwaniec, A. Holovatyy, V. Teslyuk, M. Lobur, K. Kolesnyk, M. Mashevska, Development of vibration spectrum analyzer using the raspberry pi microcomputer and 3-axis digital mems accelerometer adxl345. in *2017 XIIIth International Conference on Perspective Technologies and Methods in MEMS Design (MEMSTECH)* (IEEE, 2017), pp. 25–29
46. A. Jabłoński, M. Żegleń, W. Staszewski, P. Czop, T. Barszcz, How to build a vibration monitoring system on your own?. in *Advances in Condition Monitoring of Machinery in Non-Stationary Operations* (Springer, 2018), pp. 111–121
47. O. Janssens, V. Slavkovikj, B. Vervisch, K. Stockman, M. Loccufier, S. Verstockt, R. Van de Walle, S. Van Hoecke, Convolutional neural network based fault detection for rotating machinery. J. Sound Vib. **377**, 331–345 (2016)

48. Q. Jiang, B.W. Suter, Instantaneous frequency estimation based on synchrosqueezing wavelet transform. Signal Process. **138**, 167–181 (2017)
49. X. Jiang, S. Mahadevan, H. Adeli, Bayesian wavelet packet denoising for structural system identification. Struct. Control Health Monit. **14**(2), 333–356 (2007)
50. Y. Jiang, H. Zhu, Z. Li, A new compound faults detection method for rolling bearings based on empirical wavelet transform and chaotic oscillator. Chaos Solitons Fract. **89**, 8–19 (2016)
51. Z. Jianwei, Z. Lianghuan, J. Qi, Z. Yu, G. Jia, Research on operating modal parameter identification for high dam discharge structure based on the hilbert-huang transform. J. Vib. Meas. Diag **4**, 32 (2015)
52. R. Johansson, *Signal Processing* (Apress, Berkeley, 2019), pp. 573–599
53. S. Kaloni, M. Shrikhande, Output only system identification based on synchrosqueezed transform. Procedia Eng. **199**, 1002–1007 (2017)
54. R.H. Landau, M.J. Páez, C.C. Bordeianu, *Computational physics: problem solving with Python* (Wiley, New York, 2015)
55. G. Lee, F. Wasilewski, R. Gommers, K. Wohlfahrt, A. O'Leary, H. Nahrstaedt, Pywavelets: Wavelet transforms in python (2006)
56. Y. Lei, J. Lin, Z. He, M.J. Zuo, A review on empirical mode decomposition in fault diagnosis of rotating machinery. Mech. Syst. Signal Process. **35**(1-2), 108–126 (2013)
57. V.C. Leite, J.G.B. da Silva, G.F.C. Veloso, L.E.B. da Silva, G. Lambert-Torres, E.L. Bonaldi, de Oliveira L.E.d.L., Detection of localized bearing faults in induction machines by spectral kurtosis and envelope analysis of stator current. IEEE Trans. Ind. Electron. **62**(3), 1855–1865 (2014)
58. C. Li, M. Liang, A generalized synchrosqueezing transform for enhancing signal time–frequency representation. Signal Process. **92**(9), 2264–2274 (2012)
59. L. Li, H. Cai, H. Han, Q. Jiang, H. Ji, Adaptive short-time fourier transform and synchrosqueezing transform for non-stationary signal separation. Signal Process. **166**, 107231 (2020)
60. L. Li, H. Cai, Q. Jiang, Adaptive synchrosqueezing transform with a time-varying parameter for non-stationary signal separation. Appl. Comput. Harmon. Anal. **49**(3), 1075–1106 (2020)
61. L. Li, F. Wang, F. Shang, Y. Jia, C. Zhao, D. Kong, Energy spectrum analysis of blast waves based on an improved hilbert–huang transform. Shock Waves **27**(3), 487–494 (2017)
62. Z. Li, H.S. Park, H. Adeli, New method for modal identification of super high-rise building structures using discretized synchrosqueezed wavelet and hilbert transforms. Struct. Des. Tall Spec. Build. **26**(3), e1312 (2017)
63. Z. Liang, J. Liang, L. Zhang, C. Wang, Z. Yun, X. Zhang, Analysis of multi-scale chaotic characteristics of wind power based on hilbert–huang transform and hurst analysis. Appl. Energy **159**, 51–61 (2015)
64. H. Liu, W. Huang, S. Wang, Z. Zhu, Adaptive spectral kurtosis filtering based on morlet wavelet and its application for signal transients detection. Signal Process. **96**, 118–124 (2014)
65. S. Liu, G. Tang, X. Wang, Y. He, Time-frequency analysis based on improved variational mode decomposition and teager energy operator for rotor system fault diagnosis. Math. Probl. Eng. **2016** (2016)
66. Z. Liu, Q. Zhang, An approach to recognize the transient disturbances with spectral kurtosis. IEEE Trans. Instrum. Meas. **63**(1), 46–55 (2013)
67. J. Lu, Q. Jiang, L. Li, Analysis of adaptive synchrosqueezing transform with a time-varying parameter. Adv. Comput. Math. **46**(5), 1–40 (2020)
68. S.H. Mahdavi, H. Abdul Razak, A comparative study on optimal structural dynamics using wavelet functions. Math. Probl. Eng., 2015 (2015)
69. R.U. Maheswari, R. Umamaheswari, Trends in non-stationary signal processing techniques applied to vibration analysis of wind turbine drive train–a contemporary survey. Mech. Syst. Signal Process. **85**, 296–311 (2017)
70. J.M. Mahoney, R. Nathan, Mechanical vibrations modal analysis project with arduinos. in *ASEE Annual Conference and Exposition, Conference Proceedings*, Vol. 2017, (2017)
71. S. Mallat, *A wavelet tour of signal processing: the sparse way* (Academic Press, Cambridge, 2008)
72. W. Martin, P. Flandrin, Wigner-ville spectral analysis of nonstationary processes. IEEE Trans. Acoust. Speech Signal Process. **33**(6), 1461–1470 (1985)
73. C. Mateo, J.A. Talavera, Short-time fourier transform with the window size fixed in the frequency domain. Digit. Signal Process. **77**, 13–21 (2018)
74. M. Mihalec, J. Slavič, M. Boltežar, Synchrosqueezed wavelet transform for damping identification. Mech. Syst. Signal Process. **80**, 324–334 (2016)
75. L.A. Montejo, A.L. Vidot-Vega, Synchrosqueezed wavelet transform for frequency and damping identification from noisy signals. Smart Struct. Syst. **9**(5), 441–459 (2012)
76. A.H. Nayfeh, D.T. Mook, *Nonlinear oscillations* (Wiley, New York, 2008)
77. J.P. Noël, G. Kerschen, Nonlinear system identification in structural dynamics: 10 more years of progress. Mech. Syst. Signal Process. **83**, 2–35 (2017)
78. J. Nunez-Iglesias, S. Van Der Walt, S. Walt, H. Dashnow, *Elegant SciPy: The art of scientific python* (O'Reilly Media Inc., Sebastopol, 2017)
79. T. Oberlin, S. Meignen, V. Perrier, The fourier-based synchrosqueezing transform. in *2014 IEEE International Conference on Acoustics, Speech and Signal Processing (ICASSP)* (IEEE, 2014), pp. 315–319
80. V. Ondra, I.A. Sever, C.W. Schwingshackl, Non-linear system identification using the hilbert-huang transform and complex non-linear modal analysis. in *Nonlinear Dynamics*, Vol. 1 (Springer, 2017), pp. 77–86
81. P.F. Pai, Nonlinear vibration characterization by signal decomposition. J Sound Vib. **307**(3-5), 527–544 (2007)
82. A. Pajankar, Signal processing with scipy. in *Raspberry Pi Supercomputing and Scientific Programming* (Springer, 2017), pp. 139–147
83. F. Peñaranda, V. Naranjo, R. Verdu-Monedero, G.R. Lloyd, J. Nallala, N. Stone, Multimodal registration of optical microscopic and infrared spectroscopic images from different tissue sections: An application to colon cancer. Digit. Signal Process. **68**, 1–15 (2017)
84. C.A. Perez-Ramirez, J.P. Amezquita-Sanchez, H. Adeli, M. Valtierra-Rodriguez, D. Camarena-Martinez, R.J. Romero-Troncoso, New methodology for modal parameters identification of smart civil structures using ambient vibrations and synchrosqueezed wavelet transform. Eng. Appl. Artif. Intel. **48**, 1–12 (2016)
85. V. Piccirillo, J.M. Balthazar, A.M. Tusset, D. Bernardini, G. Rega, Characterizing the nonlinear behavior of a pseudoelastic oscillator via the wavelet transform. Proc. Inst. Mech. Eng. Pt. C J. Mechan. Eng. Sci. **230**(1), 120–132 (2016)
86. A.D. Poularikas, *Understanding digital signal processing with MATLAB® and solutions* (CRC Press, Boca Raton, 2017)
87. Z. Průša, P.L. Søndergaard, N. Holighaus, C. Wiesmeyr, P. Balazs, The large time-frequency analysis toolbox 2.0. in

International Symposium on Computer Music Multidisciplinary Research (Springer, 2013), pp. 419–442

88. H. Qu, T. Li, G. Chen, Multiple analytical mode decompositions (m-amd) for high accuracy parameter identification of nonlinear oscillators from free vibration. Mech. Syst. Signal Process. **117**, 483–497 (2019)
89. R. Randall, Applications of spectral kurtosis in machine diagnostics and prognostics. in *Key Engineering Materials*, Vol. 293 (Trans Tech Publ, 2005), pp. 21–32
90. J.L. Rojo-Álvarez, M. Martínez-Ramón, J.M. Marí, G. Camps-Valls, *Digital signal processing with Kernel methods* (Wiley Online Library, New York, 2018)
91. F. Romberg, High-resolution time-frequency analysis of neurovascular responses to ischemic challenges (2012)
92. A. Sarrafi, Z. Mao, Statistical modeling of wavelet-transform-based features in structural health monitoring. in *Model Validation and Uncertainty Quantification*, Vol. 3 (Springer, 2016), pp. 253–262
93. R. Shanmugam, R. Chattamvelli, *Statistics for scientists and engineers* (Wiley Online Library, New York, 2015)
94. Y.L. Sheu, L.Y. Hsu, P.T. Chou, H.T. Wu, Entropy-based time-varying window width selection for nonlinear-type time–frequency analysis. Int. J. Data Sci. Anal. **3**(4), 231–245 (2017)
95. H.G. Stark, *Wavelets and signal processing: an application-based introduction* (Springer Science & Business Media, New York, 2005)
96. J. Stark, B.V. Arumugam, Extracting slowly varying signals from a chaotic background. Int. J. Bifur. Chaos **2**(02), 413–419 (1992)
97. R.G. Stockwell, L. Mansinha, R. Lowe, Localization of the complex spectrum: the s transform. IEEE Trans. Signal Process. **44**(4), 998–1001 (1996)
98. A. Teolis, Signal representation and frames. in *Computational Signal Processing with Wavelets* (Springer, 2017), pp. 29–57
99. G. Thakur, E. Brevdo, N.S. Fučkar, H.T. Wu, The synchrosqueezing algorithm for time-varying spectral analysis:, Robustness properties and new paleoclimate applications. Signal Process. **93**(5), 1079–1094 (2013)
100. G. Thakur, H.T. Wu, Synchrosqueezing-based recovery of instantaneous frequency from nonuniform samples. SIAM J. Math. Anal. **43**(5), 2078–2095 (2011)
101. C. Tong, X. Chen, S. Wang, Nonlinear squeezing wavelet transform for rotor rub-impact fault detection. in *Model Validation and Uncertainty Quantification*, Vol. 3 (Springer, 2019), pp. 21–29
102. M. Varanis, J. Balthazar, A. Silva, A. Mereles, R. Pederiva, Remarks on the sommerfeld effect characterization in the wavelet domain. J. Vib. Control. **25**(1), 98–108 (2019)
103. M. Varanis, J.P. Norenberg, R. Tumolin Rocha, C. Oliveira, J. Balthazar, A. Tusset, Nonlinear dynamics and chaos of the portal frame model as an energy harvester: A time-frequency analysis approach. Sapienza University of Rome (2019)
104. M. Varanis, J.P.C. Norenberg, R.T. Rocha, C. Oliveira, J.M. Balthazar, Â.M. Tusset, A comparison of time-frequency methods for nonlinear dynamics and chaos analysis in an energy harvesting model. Braz. J. Phys., 1–10 (2020)
105. M. Varanis, R. Pederiva, Wavelet time-frequency analysis with daubechies filters and dimension reduction methods for fault identification induction machine in stationary operations. in *Proceedings of the 23rd ABCM International Congress of Mechanical Engineering (Cobem2015)*, (2015)
106. M. Varanis, R. Pederiva, The influence of the wavelet filter in the parameters extraction for signal classification: An experimental study. Proc. Ser. Braz. Soc. Comput. Appl. Math. **5**(1) (2017)
107. M. Varanis, R. Pederiva, Statements on wavelet packet energy–entropy signatures and filter influence in fault diagnosis of induction motor in non-stationary operations. J. Braz. Soc. Mech. Sci. Eng. **40**(2), 98 (2018)
108. M. Varanis, A. Silva, A. Mereles, R. Pederiva, Mems accelerometers for mechanical vibrations analysis: a comprehensive review with applications. J. Braz. Soc. Mech. Sci. Eng. **40**(11), 527 (2018)
109. M. Varanis, A.L. Silva, P.H.A. Brunetto, R.F. Gregolin, Instrumentation for mechanical vibrations analysis in the time domain and frequency domain using the arduino platform. Revista Brasileira de Ensino de Física **38**(1) (2016)
110. M. Varanis, A.L. Silva, A. Mereles, C. de Oliveira, J.M. Balthazar, Instrumentation of a nonlinear pendulum using arduino. Revista Interdisciplinar de Pesquisa em Engenharia **2**(27)
111. M. Varanis, A.L. Silva, A.G. Mereles, On mechanical vibration analysis of a multi degree of freedom system based on arduino and mems accelerometers. Revista Brasileira de Ensino de Física **40**(1) (2018)
112. M.V. Varanis, A.M. Tusset, J.M. Balthazar, G. Litak, C. Oliveira, R.T. Rocha, A. Nabarrete, V. Piccirillo, Dynamics and control of periodic and non-periodic behavior of duffing vibrating system with fractional damping and excited by a non-ideal motor. J. Franklin Inst. (2019)
113. V. Vrabie, P. Granjon, C. Serviere, Spectral kurtosis: from definition to application. in *6th IEEE International Workshop on Nonlinear Signal and Image Processing (NSIP 2003)*, (2003)
114. A. Vretblad, Vol. 223, *Fourier analysis and its applications* (Springer Science & Business Media, New York, 2003)
115. S. Wang, X. Chen, G. Cai, B. Chen, X. Li, Z. He, Matching demodulation transform and synchrosqueezing in time-frequency analysis. IEEE Trans. Signal Process. **62**(1), 69–84 (2014)
116. S. Wang, W. Huang, Z. Zhu, Transient modeling and parameter identification based on wavelet and correlation filtering for rotating machine fault diagnosis. Mech. Syst. Signal Process. **25**(4), 1299–1320 (2011)
117. S. Wang, L. Yang, X. Chen, C. Tong, B. Ding, J. Xiang, Nonlinear squeezing time-frequency transform and application in rotor rub-impact fault diagnosis. J. Manuf. Sci. Eng. **139**(10), 101005 (2017)
118. Y. Wang, J. Xiang, R. Markert, M. Liang, Spectral kurtosis for fault detection, diagnosis and prognostics of rotating machines: A review with applications. Mech. Syst. Signal Process. **66**, 679–698 (2016)
119. Z.C. Wang, D. Geng, W.X. Ren, G.D. Chen, G.F. Zhang, Damage detection of nonlinear structures with analytical mode decomposition and hilbert transform. Smart Struct. Syst. **15**(1), 1–13 (2015)
120. Z.C. Wang, W.X. Ren, Parameter identification of closely spaced structural modals based on analytical mode decomposition. Noise Vib. Control **6**, 6 (2013)
121. A. Widodo, B.S. Yang, Wavelet support vector machine for induction machine fault diagnosis based on transient current signal. Expert Syst. Appl. **35**(1-2), 307–316 (2008)
122. H.T. Wu, Adaptive analysis of complex data sets. Ph.D. thesis, Princeton University (2012)
123. H.T. Wu, P. Flandrin, I. Daubechies, One or two frequencies? the synchrosqueezing answers. Adv. Adapt. Data Anal. **3**(01n02), 29–39 (2011)
124. J.W. Wu, H.B. Bao, Nonlinear dynamics in semiconductor quantum dot laser subject to double delayed feedback: Numerical analysis. Braz. J. Phys. **50**(5), 594–601 (2020)
125. J. Xiang, Y. Zhong, A two-step method using duffing oscillator and stochastic resonance to detect mechanical faults. in *2016 IEEE International Instrumentation*

and Measurement Technology Conference Proceedings. https://doi.org/10.1109/I2MTC.2016.7520335, (2016), pp. 1–6

126. W. Xiang-Li, W. Wen-Bo, Harmonic signal extraction from noisy chaotic interferencebased on synchrosqueezed wavelet transform. Chin. Phys. B **24**(8), 080203 (2015)
127. R. Yan, R.X. Gao, X. Chen, Wavelets for fault diagnosis of rotary machines: A review with applications. Signal Process. **96**, 1–15 (2014)
128. K. Zhang, X. Chen, L. Liao, M. Tang, J. Wu, A new rotating machinery fault diagnosis method based on local oscillatory-characteristic decomposition. Digit. Signal Process. **78**, 98–107 (2018)
129. Y. Zhao, H. Cui, H. Huo, Y. Nie, Application of synchrosqueezed wavelet transforms for extraction of the oscillatory parameters of subsynchronous oscillation in power systems. Energies **11**(6), 1525 (2018)
130. R. Zhou, W. Bao, N. Li, X. Huang, D. Yu, Mechanical equipment fault diagnosis based on redundant second generation wavelet packet transform. Digit. Signal Process. **20**(1), 276–288 (2010)

Publisher's Note Springer Nature remains neutral with regard to jurisdictional claims in published maps and institutional affiliations.